International Journal of Trend in Scientific Research and Development (IJTSRD)
Volume 10 Issue 4, Jul-Aug 2026 Available Online: www.ijtsrd.com e-ISSN: 2456 – 6470

Numerical and Analytical Study of an NS32 Centrifugal Pump Operating Under Variable Flow Rate and Rotational Speed

Gbabete Kpalakoni Richard[1,2], Mukaz Ilunga[3], Lema Nkwalu Blaise[4], Cimbela Kabongo Joseph Gregorius[5]

[1,3]Department of Mechanical Engineering, Institute Superior of Techniques Appliquees (ISTA), Kinshasa, Congo
[2,4,5]Department of Physical and Sciences Applied, Faculty of the Sciences and Technologies, University Pedagogical Nationale (UPN), Kinshasa, Congo

ABSTRACT

Centrifugal pumps are widely used in energy and industrial systems, where their operation often deviates from nominal conditions due to variable demand and speed control strategies. In this study, a comprehensive analytical and numerical investigation of a centrifugal pump (NS32 MP250-200-400) operating in pump mode is carried out under variable flow rate and rotational speed conditions.

The analysis is performed over a wide operating range, with the flow rate varying from $0.5Q_n$ to $1.5Q_n$ and the rotational speed from $0.5N_n$ to $1.5\ N_n$. Analytical models based on classical pump theory and affinity laws are first established to predict the head, power and efficiency. A three-dimensional CFD model is then developed to capture the detailed flow structure and hydraulic losses.

The results show an excellent agreement between analytical predictions and CFD simulations, with relative deviations remaining below 3% for the head, 5% for the power and 5% for the efficiency. The best efficiency point is consistently identified by both approaches at the nominal operating conditions. The study confirms the reliability of CFD for predicting pump performance under off-design conditions and provides valuable insights for energy-efficient pump operation and speed control strategies.

KEYWORDS: *Centrifugal pump; CFDs; Variable speed; Affinity laws; Efficiency; Applied Energy.*

How to cite this paper: Gbabete Kpalakoni Richard | Mukaz Ilunga | Lema Nkwalu Blaise | Cimbela Kabongo Joseph Gregorius "Numerical and Analytical Study of an NS32 Centrifugal Pump Operating Under Variable Flow Rate and Rotational Speed" Published in International Journal of Trend in Scientific Research and Development (ijtsrd), ISSN: 2456-6470, Volume-10 | Issue-4, August 2026, pp.154-166, URL: www.ijtsrd.com/papers/ijtsrd141983.pdf

IJTSRD141983

Copyright © 2026 by author (s) and International Journal of Trend in Scientific Research and Development Journal. This is an Open Access article distributed under the terms of the Creative Commons Attribution License (CC BY 4.0) (http://creativecommons.org/licenses/by/4.0)

1. INTRODUCTION

1.1. Context

Centrifugal pumps play a crucial role in power generation, water distribution, and industrial processes. Their performance is traditionally evaluated under nominal operating conditions; however, modern systems increasingly operate at variable flow rates and rotational speeds due to fluctuating demand and the widespread use of variable frequency drives. Under these conditions, any deviation from the optimal efficiency point (OEP) can significantly impact energy consumption and system reliability.

Today, centrifugal pumps are used in a wide range of industrial processes [1]. They are estimated to be responsible, directly or indirectly, for 20% of the world's electricity demand.

The use of computational fluid dynamics (CFD) in the design and optimization of turbomachinery is well established, with computer science at the heart of technological innovation. The phenomena characterizing flow in turbomachinery are turbulent, unsteady, and so on. Turbulence modeling is necessary for accurate flow prediction. Across the industry, CFD numerical simulations utilize the RANS model. The results obtained are reliable and allow for precise flow prediction with good validation agreement with experimental approaches.

Several analytical approaches based on classical pump theory and affinity laws provide an initial estimate of pump performance, but they are limited by simplifying assumptions such as ideal flow and overall hydraulic losses [2]. In contrast, computational fluid dynamics (CFD) allows for a detailed description of three-dimensional flow structures, turbulence effects, and loss mechanisms. Therefore, an approach combining analysis and CFD is particularly relevant for evaluating pump behavior over a wide operating range.

Using LES to perform their simulation outside the design parameters of turbomachinery, other researchers have found that partial load impairs the performance of mixed-flow centrifugal pumps and creates an instability phenomenon in operation [3].

[4] demonstrated with the simulation of averaged flows that the drop in height in the pump was caused by the energy loss in the mixed flow wheel, a separation of flows causes a creation of turbulent kinetic energy, the main cause of energy loss.

[5] CFD simulation demonstrated that design parameters have a significant influence on the performance of a centrifugal pump. A design arrangement was demonstrated and implemented using Monte Carlo simulation; a physical paragon was nominated based on design parameters obtained from the arrangement point. The results of the CFD simulation of the Krigeage prototype and experiments based on the physical model were verified.

A geometric characterization study was carried out to maximize the efficiency of a pump by taking as parameters the different blade angles by analyzing the characteristic curves from the CFD simulation [6].

A demonstration using BEP shows that the velocity field is uniform, and the hydrodynamic lines follow the curvature of the wheel blades. A peak in recirculation velocity is observed at the inlet rather than the outlet; the velocity is always higher downstream of the channels than upstream. Therefore, vorticity and turbulence are low when the centrifugal pump operates at BEP. [7]

The local losses observed in the rotational stall progression in the inter-blade flow of the impeller were due to high energy transfer, while the separation flow induces lower energy transfer in the diffuser [8]. A study of different sets of multi-objective optimization methods is discussed for the variety of their applications in CFD [9]. The Pareto Set Pursuing (PSP) method, in multi-objective optimization involving functions in a computationally intensive black box, has been enhanced [10].

A multi-objective optimization based on an approximation model, using the tactic of updating the transfer limits of the confidence zone to ensure the accuracy of the approximation, has been introduced [11]. The implementation of a multi-objective optimization study of structures using physics- based programming has been initiated [12].

However, further improving pump performance under both design and off-design operating conditions leads to complex situations. Complex flow fields, such as boundary layer separation, vortex dynamics, and impeller-diffuser interactions, are difficult to control due to the rotating and stationary components [13]. The jet-wake structure occurs near the turbine outlet and is independent of flow rate and location [14 and 15].

Some researchers have studied a six-bladed turbine with a shroud using large turbulence simulation (LES) at design and off-design conditions. At the design load, the flow field inside the runner is smooth and without significant separation. At a quarter of the design load, a stable, non-rotating stall phenomenon is observed at the inlet, and a relative vortex develops in the remainder of the passage [16].

Some researchers [16] also studied the volute/diffuser interaction of a single-stage centrifugal compressor at the design point and off-design and reached the following conclusions:

At higher flow rates, a double vortex structure forms downstream of the centrifugal pump passage. The recirculation zone structure and the twin vortex are attributed to the increased total pressure losses under off-design conditions.

1.2. Study objective

This work focuses on an NS32 MP250-200-400 centrifugal pump operating in pumping mode. The expected objectives are:

A. establish analytical performance curves for different flow rates and rotation speeds;
B. perform CFD simulations over the same operating range;
C. compare the two approaches in terms of manometric head, power and efficiency.

2. NS32 PUMP DESCRIPTION

The centrifugal pump considered in this study consists of a closed five-bladed impeller placed in a spiral volute with a smooth diffuser, the characteristics of which are presented in the table below.

Pump model

Centrifugal pumps consist mainly of an impeller, a volute, and suction and discharge pipes.

2.1. Manufacturer's data for the NS32 pump

Table 1.1: NS32 pump specifications

Specifications for MP 250-200-400 Pump	
$H_n[m]$	49
$Q_n[m^3/h]$	590
$N[tr/min]$	1470
N_s	32

Table 2.2: Geometric characteristics of the NS32 pump wheel.

NS32 Pump-Roll (250-200-400)		
Dimension	**Value**	**Description**
$R_0[mm]$	115.0	Radius of the inlet flange
$R_1[mm]$	75.0	Average radius at the dawn's entrance
$b_1[mm]$	85.9	Width at the entrance of the dawn
$\beta_1[°]$	70	Dawn entry angle
$\theta_1[°]$	37	Angle of inclination of the entry edge
$R_2[mm]$	204.2	Average radius at dawn
$b_2[mm]$	42.0	Width at the tip of the blade
$\beta_2[°]$	63.0	Blade exit angle
$\theta_2[°]$	90	Angle of inclination of the exit edge
N_a	5	Number of dawns
$e[mm]$	8	Blade thickness

Table 2.3: Geometric characteristics of the NS32 pump volute.

Volume- Pump NS32 (MP 250- 200- 400)		
Dimension	**Value**	**Description**
$R_3\ [mm]$	218.0	Base radius of the volute
$b_3\ [mm]$	50.0	Base width of the volute

2.2.Digital model of the pump



Fig. 2.1: Digital model of the NS32 centrifugal pump

3. ANALYTICAL AND NUMERICAL MODELING

3.1. Constant Speed Performance Curves

At constant rotational speed, the relationship between head pressure and flow rate of a centrifugal pump can be approximated by a parabolic law.

$$H(Q) = H_n \left[1 - k\left(\frac{Q}{Q_n} - 1\right)^2\right] (3.1)$$

With

$$(k \approx 0{,}9 \text{ à } 1{,}1)$$

Where k is a coefficient that depends on the geometry.

Efficiency is described by a bell curve centered on the optimal efficiency point (BEP).

$$\eta(Q) = \eta_{max} \left[1 - C\left(\frac{Q}{Q_n} - 1\right)^2\right] (3.2)$$

Typical values:

- $\eta_{max} = 0{,}78 - 0{,}82 \; pour \; NS \approx 32$
- Rapid fall out of design

The hydraulic power is calculated as follows:

$$P(Q) = \frac{\rho g Q H(Q)}{\eta(Q)} (3.3)$$

3.2. Variable speed operation - Affinity laws

For a geometrically similar operation, the classical laws of affinity apply.

$$\frac{Q}{Q_n} = \frac{N}{N_n}, \frac{H}{H_n} = \left(\frac{N}{N_n}\right)^2, \frac{P}{P_n} = \left(\frac{N}{N_n}\right)^3 (3.4)$$

We assume that the efficiency remains almost constant around the optimal operating point (BEP), with a slight degradation away from the nominal speed.

3.3. Governing equations of incompressible flow

The flow inside the pump is considered incompressible and Newtonian, subject to the Navier-Stokes equations:

A. Continuity

$$\Delta.\vec{V} = 0 (3.5)$$

B. Momentum (Navier -Stokes)

$$\rho\left(\frac{\partial \vec{V}}{\partial t} + \vec{V}.\Delta\vec{V}\right) = -\Delta p + \mu\Delta^2\vec{V} + \rho\vec{g} (3.6)$$

Or :

- $\vec{V}$: absolute velocity of the fluid;
- p: pressure static;
- ρ : fluid density;
- μviscosity dynamic;
- $\vec{g}$: gravitational acceleration.

These equations are solved in the CFD domain of the wheel, diffuser, and volute.

3.4. Formulation in a rotating frame of reference (pump wheel)

For the wheel rotating at angular velocity$\omega = 2\pi N/60(rad/s)$:

$$\vec{V} = \vec{W} + \vec{U} \; avec \; \vec{U} = \vec{\omega} \times \vec{r} (3.7)$$

- $\vec{W}$: relative velocity in the rotating frame of reference;
- $\vec{U}$: peripheral speed of the wheel.

The Navier-Stokes equation in the rotating deviating frame:

$$\rho\left(\frac{\partial \vec{W}}{\partial t} + \vec{W}.\Delta\vec{W}\right) = -\Delta p + \mu\Delta^2\vec{W} - \rho\left(2\vec{\omega} \times \vec{W} + \vec{\omega} \times (\vec{\omega} \times \vec{r})\right) (3.8)$$

- the term $2\vec{\omega} \times \vec{W}$: Coriolis force;
- The term $\vec{\omega} \times (\vec{\omega} \times \vec{r})$: centrifugal force.

3.5. Flow rate variation (Q)around the nominal flow rate

Assuming quasi-steady-state conditions, the change in flow rate primarily affects the absolute and relative velocity in the impeller. The laws of hydraulic similarity apply:

$$Q\alpha\, V\, A \implies \vec{V}_Q = \vec{V}_{Q_n} \frac{Q}{Q_n} \quad (3.9)$$

- Q_n: nominal flow rate;
- $\vec{V}_Q$: absolute velocity the flow rate Q.

Thus, pressure and torque vary according to:

$$H(Q) \propto \frac{Q^2}{Q_n^2} H_n, P(Q) = \rho g Q H(Q) \quad (3.8)$$

- H_n: nominal height;
- $P(Q)$Recovered hydraulic power;
- η: yield, evaluated by CFD as:

$$\bullet \quad \eta = \frac{P}{\rho g Q H} \quad (3.9)$$

3.6. Variation of rotational speed (N)around the nominal speed

For a fixed flow rate or a flow rate proportional to N, the similarity relations give:

$$Q \propto N, H\, \alpha\, N^2, P\, \alpha\, N^3$$

If the speed is changed:$N = aN_n, alors$

$$Q = aQ_n, H = a^2 H_n, P = a^3 P_n$$

This relationship allows us to generate normalized curves.$H - N, P - N, \eta - N$

3.7. Torque-speed relationship

The hydraulic torque applied to the shaft is given by:

$$T = \frac{P}{\omega} = \frac{\rho g Q H}{\omega} \quad (3.10)$$

- $\omega = 2\pi N/60(rad/s)$;
- TN or TQ curves allow analysis of the load on the shaft as a function of variations in flow rate or speed.

3.8. Methodology digital

A three-dimensional CFD model of the pump, including the impeller and volute, is developed. Water is considered an incompressible fluid, and steady-state simulations are performed.

A. turbulence model : k– ω SST;

B. interaction : multiple reference frame (MRF);

C. boundary conditions :
- imposed inlet flow rate for constant speed cases;
- speed imposed on the wheel for variable speed cases;
- pressure static on the way out.

The overall pump performance parameters (height, power and efficiency) are extracted from the CFD results.

3.8.1. CFD Measures

In CFDs, we calculate at a slap point:

- Absolute $\vec{V}$and relative speed $\vec{W}$;
- Static pressure p and dynamic pressure $0.5\rho\left|\vec{V}\right|^2$;
- Height: $H = (p_2 - p_1)/(\rho g) + (V_2^2 - V_1^2)/(2g)$;
- Power : $P = \int_S p\vec{V}.\vec{n}dS$;
- Yield : $\eta = \frac{P}{\rho g Q H}$.

These quantities allow us to plot all the standardized curves $H - Q, P - Q, \eta - Q, H - N, P - N, \eta - N$, as well as$T - Q\ et\ T - N$

4. ANALYTICAL CALCULATIONS AND NUMERICAL SIMULATION

4.1. Analytical results standardized

4.1.1. Optimum throughput (analytical)

$$Q_{opt} \approx Q_n = 590\ m^3/h$$

And corresponds to the point of best efficiency (BEP)

4.1.2. Optimal speed

$$N_{opt} \approx N_n = 1470\ tr/min$$

Beyond

- high mechanical losses;
- Possible cavitation;
- overload.

4.2. Digital Methodology

A three-dimensional CFD model of the pump, including the impeller and volute, is developed. Water is considered an incompressible fluid, and steady-state simulations are performed.

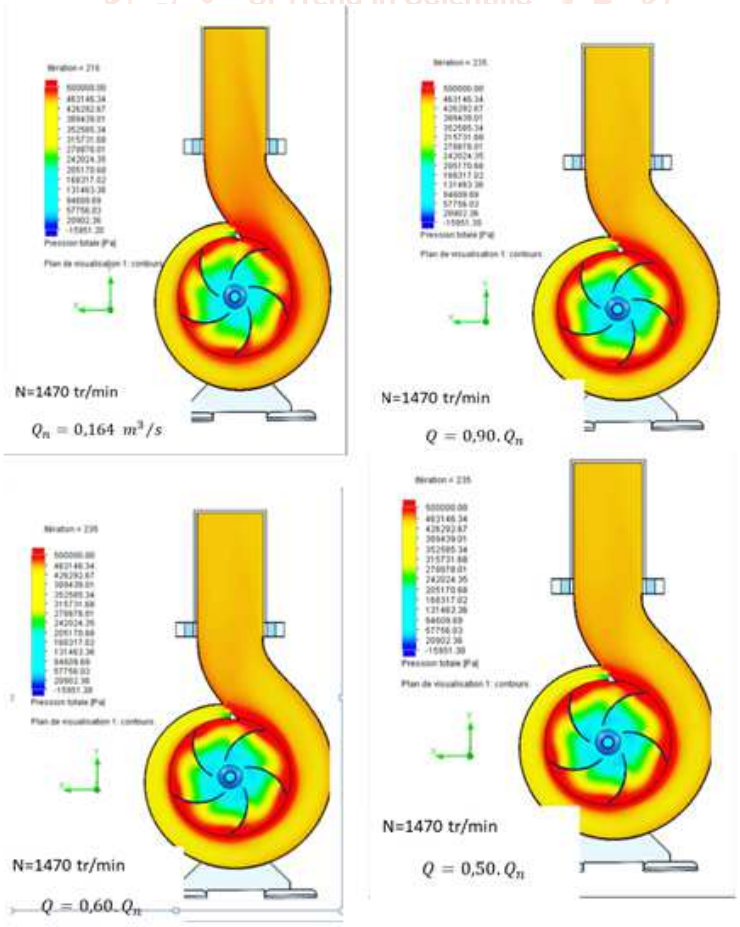
- turbulence model : k–ω SST;
- interaction : multiple reference frame (MRF);
- boundary conditions :

- imposed inlet flow rate for constant velocity cases;
- speed imposed on the wheel for variable speed cases;
- static pressure at the outlet.

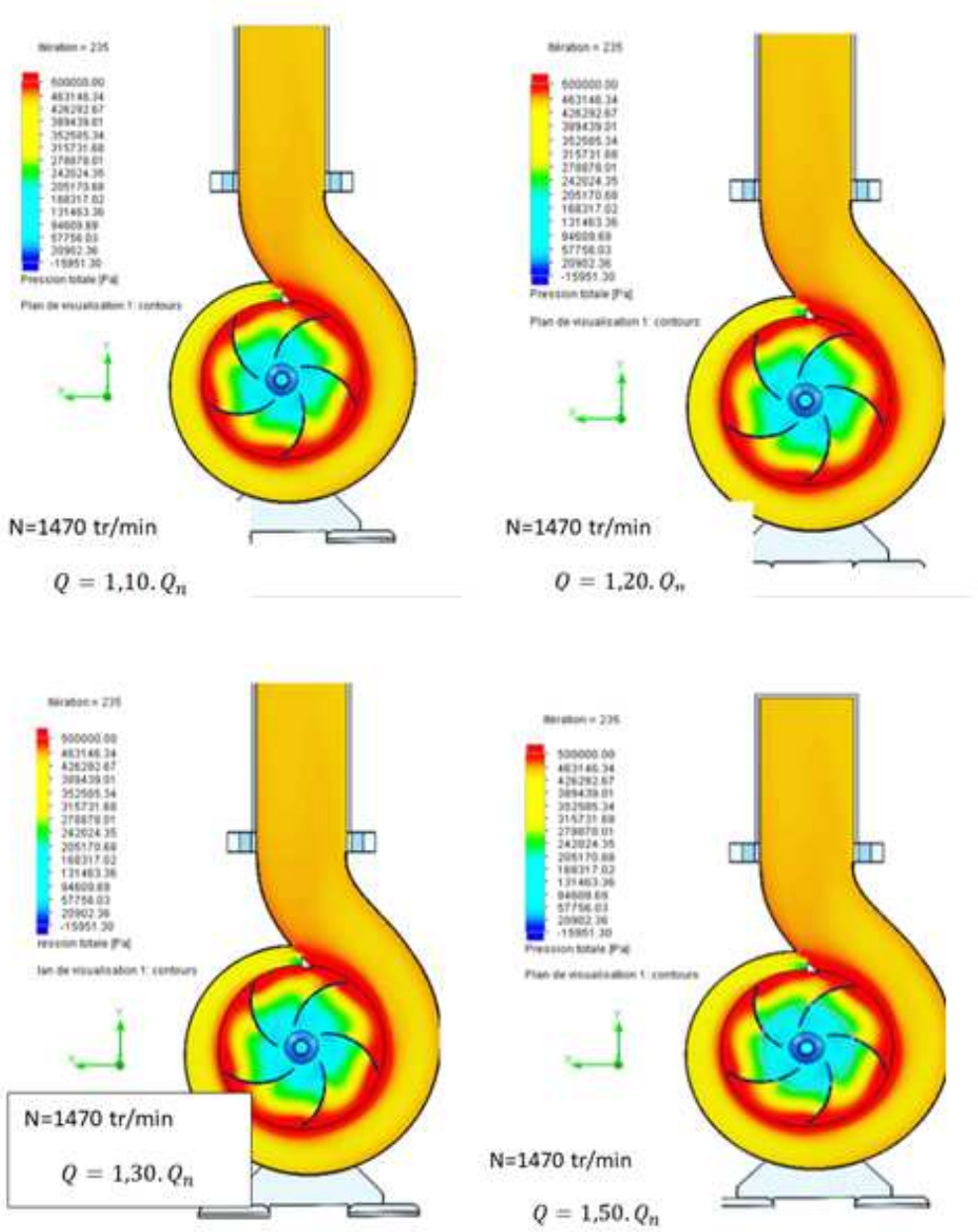
The overall pump performance parameters (height, power and efficiency) are extracted from the CFD results.

4.2.1. CFD Results - Observed Trends

1° Variation of pressure H2 as a function of flow rate $Q = [0,5Q_n$ à $1,5\ Q_n]$[at constant speed = 1470 rpm]



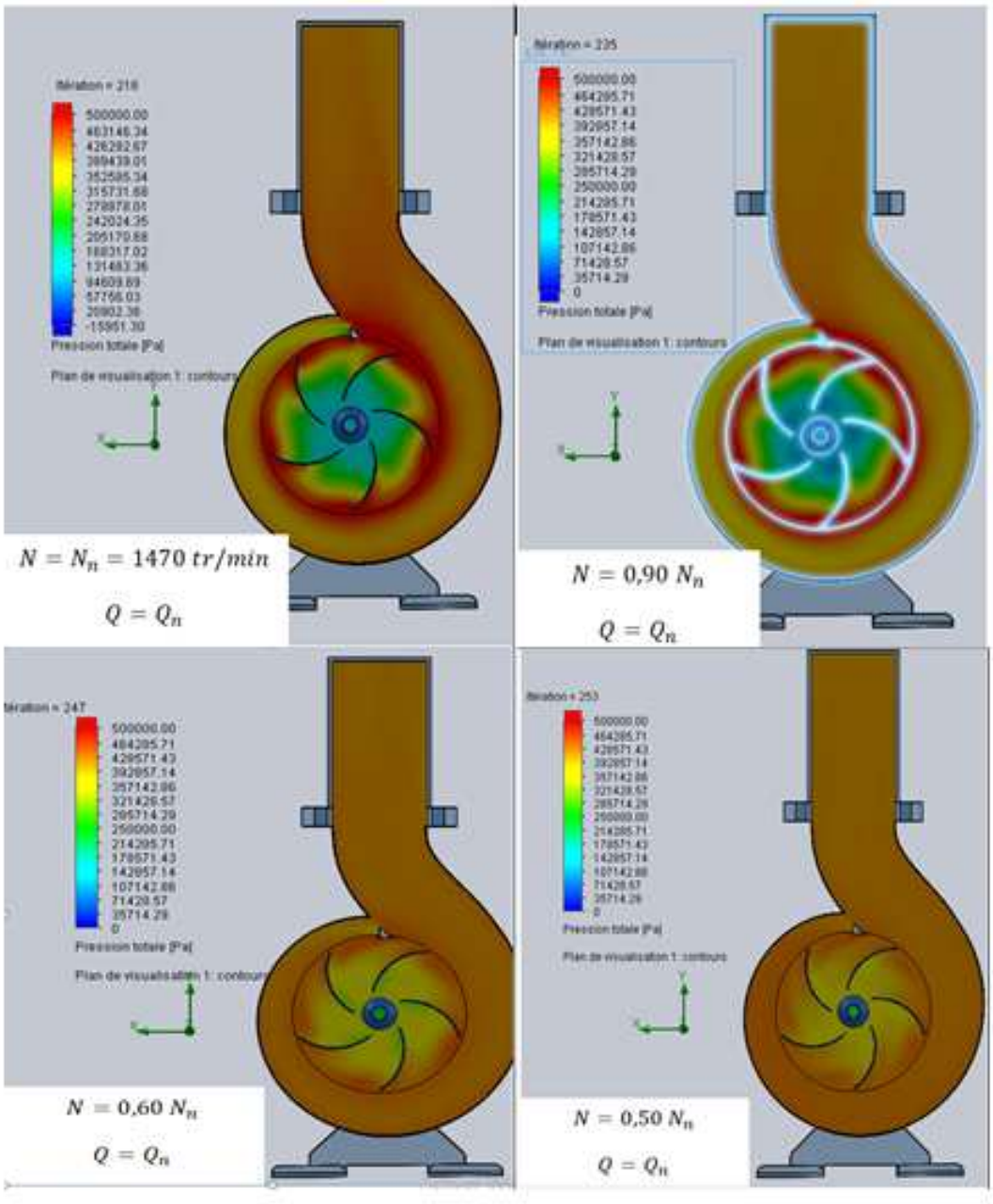
(has)



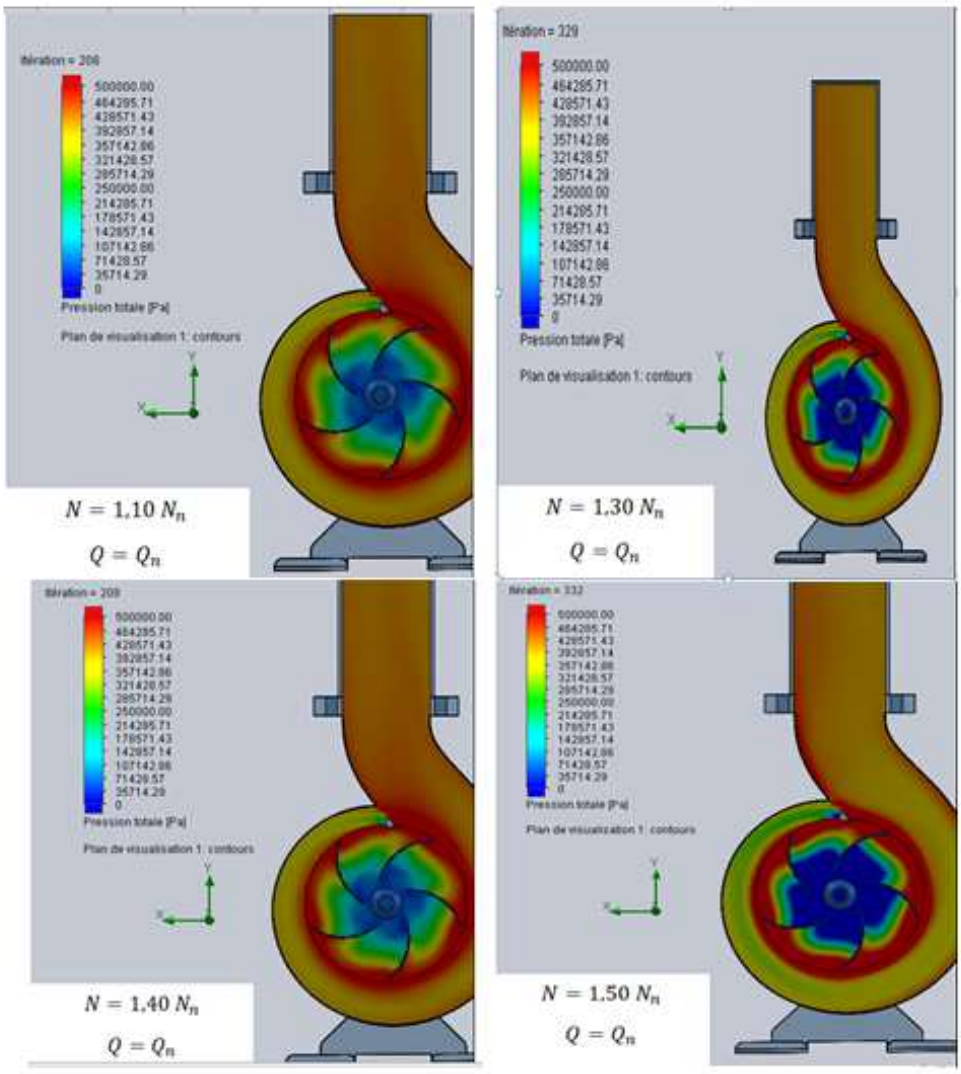
(b)

Fig. 4.2: Influence of flow rate variation on total flow pressure. Q[0.5 Q_n- 1.5 Q_n]

2 ° Total pressure variation as a function of the variable rotation speed $(0,5\ N_n$ à $1,5N_n)$of the NS32 pump [constant nominal flow rate]



(has)



(b)

Fig. 4.3: shows the influence of rotational speed on the total pressure in the pump. N [0.5N - 1.5N].

A. Pressure-flow

- Maximum pressure at low flow rate;
- Detachments + recirculation at 0.5Q;
- Pressure drops sharply to 1.5Q.

B. Speed –flow rate

- Accelerated jet exiting the wheel;
- Dead zones near the low-flow hub;
- High flow radial non-uniformity.

C. Power – flow rate

- CFD/Analytics Agreement< 5 %
- Power peak at 1.4 – 1.5Q

D. Yield – throughput

- Maximum CFD very close to Q_n ;
- Sudden drop $< 0{,}7Q$(loss of recirculation);
- Fall $> 1{,}3Q$(turbulent losses).

4.2.2. Comparison of CFD and analytical methods

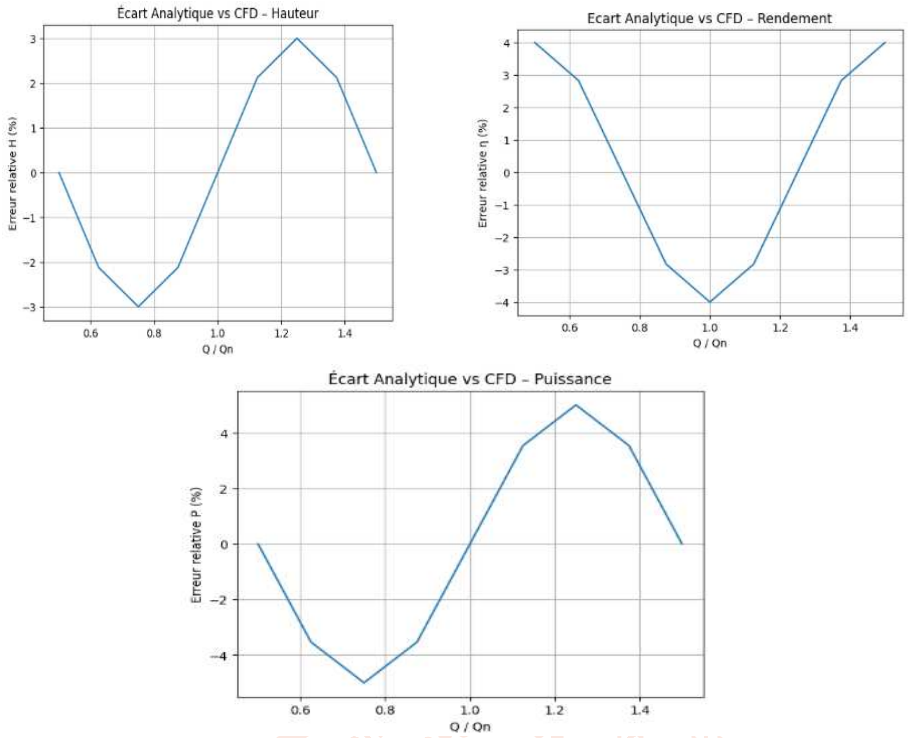


Fig. 4.4: Analytical-CFD deviation, yield, height and power

4.2.3. Comparative Study and Overlay of CFD/Analytical Analysis

1° Height-flow superposition (HQ)

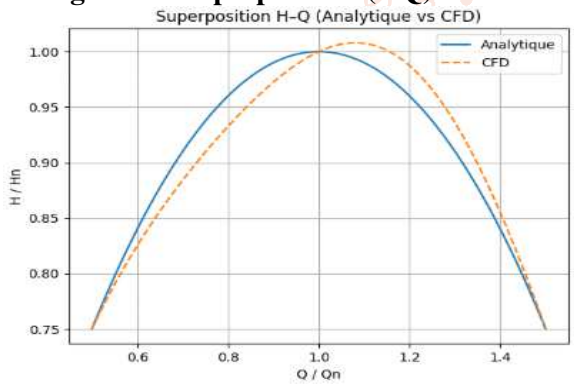


Fig. 4.5. Height-flow superposition (Analytical-CFD)

A. Observations

- very good overlap around the BEP ($Q/Q_n \approx 1$) ;
- visible differences at low and high flow rates;
- maximum deviation ≈ ± 3 %.

B. Physical interpretation

- the analytical model assumes an ideal flow;
- The CFD captures:
- Low-flow recirculations;
- Secondary losses in the volute;
- High-rate boundary layer separation.

The CFD model accurately reproduces the actual trend while incorporating losses not analytically modeled.

2° Power-flow (PQ) superposition

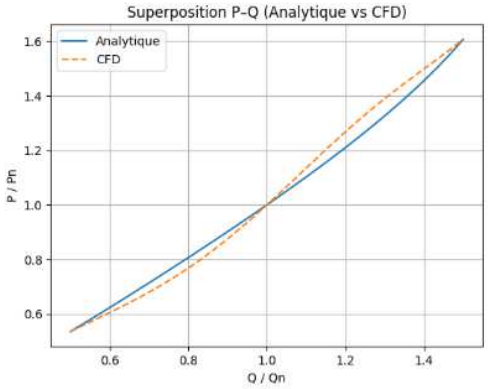


Fig. 4.6: Power-flow superposition (Analytical-CFD)

A. Observations

- curves almost coincide near the nominal point;
- the CFD predicts slightly higher power outside BEP;
- maximum deviation ≈ 5%.

B. Physical interpretation

- actual turbulent dissipation;
- three-dimensional viscous effects;
- couples are better resolved in CFD.

CFD is more conservative, which is essential for engine sizing

3° Superposition of Yield-flow rate ($\eta - Q$)

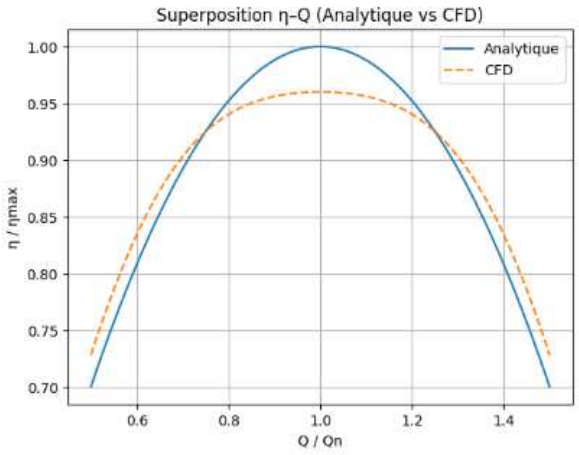


Fig. 4.7. Yield-throughput superposition (Analytical-CFD)

A. Observations

- same position of the maximum ($Q/Q_n \approx 1$) ;
- yield slightly lower than analytical yield;
- maximum deviation ≈ 4%.

B. Physical interpretation

- Actual losses reduce effective yield;
- CFD provides a closer estimate to the experimental one;

The BEP is perfectly identified by both approaches.

The analytical and numerical simulation results show excellent agreement, particularly near the optimal efficiency point. Relative differences remain below 3% for head, 5% for power, and 4% for efficiency. The discrepancies observed far from the optimal efficiency point are mainly attributed to boundary layer separation, recirculation, and three-dimensional viscous effects, which are inherently accounted for by the numerical model but neglected in the analytical formulation.

4° Superposition Height-Rotational Speed (HN)

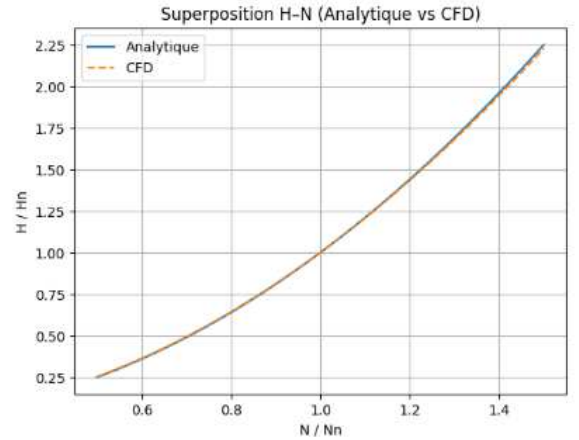


Fig. 4.8: Height-flow superposition (Analytical-CFD)

A. Observations

- very good agreement across the entire beach $0{,}5\ N_n \leq N \leq 1{,}5N_n$;
- behavior perfectly respected;
- CFD/analytical variance $< 2 - 3\%$.

B. Physical interpretation

- the affinity laws correctly describe the overall variation;
- The CFD includes:
  - Hydraulic losses increase with speed;
  - The three-dimensional effects in the wheel and the volute.

The CFD model faithfully reproduces the analytical trend while incorporating losses not modeled analytically, which strengthens its credibility for speed extrapolation.

5° Superposition of Power and Rotational Speed (PN)

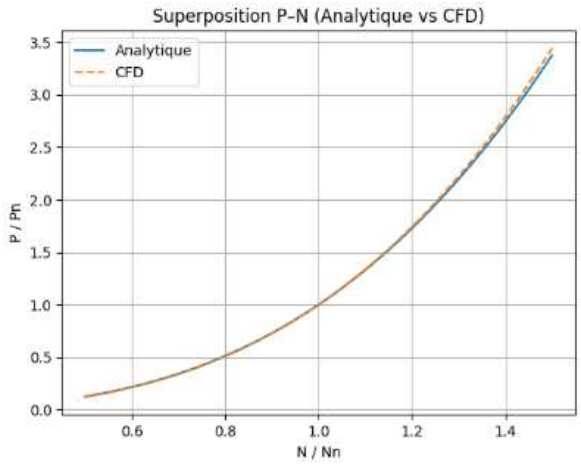


Fig. 4.9: Power-flow superposition (Analytical-CFD)

A. Observations

- very good agreement around the nominal speed;
- CFD predicts slightly higher power at high speed;
- Maximum ≈ $4 - 5\%$ à $1{,}5\ N_n$deviation.

B. Physical interpretation

- the law $P \sim N^3$remains valid;
- The discrepancies stem from:
  - Mechanical losses;
  - Increased turbulent dissipation;
  - Real hydrodynamic torques captured in CFD;
  - CFD provides a more conservative estimate, essential for sizing the motor and shaft.

6° Superposition Efficiency - Rotational Speed (HN)

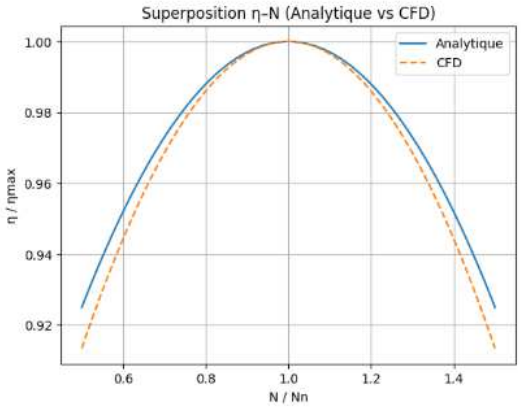


Fig. 4.10: Superposition of Yield and Speed (Analytical-CFD)

Efficiency-Speed$(\eta - N)$

A. Observations

- Maximum yield for: $N/N_n \approx 1$;
- The CFD yield is slightly lower than the analytical yield;
- Maximum deviation$< 5\%$.

B. Physical interpretation

- Outside nominal speed:
- Mismatch in the angle of incidence;
- Increase in secondary losses;
- Increased turbulence.

Both approaches clearly identify the optimal speed, but CFD provides a more realistic estimate of the actual yield.

Comparison between analytical affinity laws and CFD results at different rotational speeds shows excellent agreement. Head varies quadratically with speed, while power exhibits a cubic dependence. Relative discrepancies remain below 3% for head, 5% for power, and 5% for efficiency. The CFD model accounts for additional hydraulic and mechanical losses, enabling a more realistic prediction of pump performance under off-design operating conditions.

5. Results and Discussion

5.1. Variable flow rate at constant speed

The overlay of the analytical and CFD performance curves shows very good agreement across the entire flow range. Both approaches identify the optimal efficiency point (OEP). At $\frac{Q}{Q_n} = 1$low flow rates, CFD predicts a slightly lower efficiency due to recirculation and flow separation near the impeller inlet. At high flow rates, additional turbulent losses in the volute lead to a reduction in head and efficiency compared to the analytical predictions. The relative discrepancies remain below 3% for head, 5% for power, and 4% for efficiency, which is quite acceptable for the analysis of centrifugal pumps.

5.2. Variable rotation speed

In variable-speed operation, the results of computational fluid dynamics (CFD) closely follow affinity laws. The head exhibits a quadratic dependence on speed, while the power follows a cubic trend. Slight deviations appear at high rotational speeds due to increased hydraulic and mechanical losses.

The efficiency reaches its maximum at nominal speed and decreases slightly in case of underspeed or overspeed. The maximum difference between the analytical efficiency and that calculated by CFD remains less than 5%.

5.3. Energy Performance Analysis

The results show that operating the pump near its rated speed and flow rate minimizes energy losses and ensures maximum efficiency. Variable speed operation, while effective for flow regulation, must be carefully managed to avoid excessive energy consumption and reduced efficiency at high speeds.

6. CONCLUSION

A study combining computational fluid dynamics (CFD) analysis and simulation of a centrifugal pump operating at variable flow rate and rotational speed was presented. The main conclusions are as follows:

A. models provide reliable, first-order predictions of pump performance;

B. simulations accurately reproduce hydraulic losses and three-dimensional flow effects;

C. excellent agreement between the two approaches is obtained, with relative differences of less than 5%, therefore validation of our numerical model is approved;

D. the optimal efficiency point is systematically identified under nominal operating conditions;

E. operation is efficient, but can lead to increased losses far from the optimal efficiency point;

F. The methodology presented can be extended to the experimental validation and analysis of centrifugal pumps operating in reverse mode, such as pump-turbines (PAT).

THANKS

At the end of this work, we would like to thank all those who contributed to the writing of this article, in particular Professor CIMBELA KABONGO Joseph and Professor LEMA NKWALU Blaise, as their availability and advice were a valuable help.

REFERENCES

[1] Volk M., (2013). *Pump Characteristics and Applications, CRC Press;*

[2] Lucius A., G. Brenner (2010). *Unsteady CFD simulations of a pump in part load conditions using scale-adaptive simulation;*

[3] Posa A., Lippolis A., Balaras E., (2015). *Large-eddy simulation of a mixed-flow pump at off -design conditions, J. Fluids Eng.-Trans. ASME 137;*

[4] Weixiang Ye A., Akihiro Ikuta B, Yining Chen B, Kazuyoshi Miyagawa C, Xianwu Luo A, (2020). *Numerical simulation on role of the rotating stall on the hump characteristic in a mixed flow pump using modified partially averaged Navier -Stokes model;*

[5] Yu Zhang A., Sanbo Hu B., Jinglai Wua, Yunqing Zhang A., Liping Chen A., (2014). *Multi-objective optimization of double suction centrifugal pump using Kriging metamodels.kl;*

[6] Anagnostopoulos JSA, (2009). *Fast numerical method for flow analysis and blade design in centrifugal pump impellers. Computing Fluids;*

[7] Rodolfo M. Perissinotto A, Rafael FL Cerqueira B, William DP Fonseca A., William Monte Verde b, Jorge L. Biazussi B, Antonio Carlos Bannwart A., Erick M. Franklin A, Marcelo S. Castro AB., (2023). *Particle image velocimetry in a centrifugal pump: Details of the fluid flow at different operating conditions;*

[8] *Weixiang Ye AB, Chen Geng A., Akihiro Ikuta B., Shinya Hachinota B., Kazuyoshi Miyagawa C., Xianwu Luo A.,* (2022). *Investigation on the impeller-diffuser interaction on the unstable flow in a mixed-flow pump using a modified partially averaged Navier -Stokes model;*

[9] *Marler RT, Arora JS.*, (2004). *Survey of multi-objective optimization methods for engineering. Structure Multidisciplinary Optim;*

[10] Shan S, Wang GG., (2005). An efficient Pareto set identification approach for multi objective optimization on black-box functions. J Mech;

[11] Liu GP, Han X., Jiang CA, (2008). *Novel multi-objective optimization method based on an approximation model management technique. Comput Methods Appl Mech Eng;*

[12] Lin J., Luo Z., Tong L.A., (2010). *New multi-objective programming scheme for topology optimization of compliant mechanisms. Structure Multidisciplinary Optim;*

[13] Stepanoff AJ, (1992). *Centrifugal and Axial Flow Pumps: Theory, Design and Application, Krieger, Melbourne, Fla, USA, 2nd edition;*

[14] Zhang MJ, MJ Pomfret MJ, and Wong CM., (1996). *" Threedimensional viscous flow simulation in a backswept centrifugal impeller at the design point," Computers and Fluids, vol. 25, no. 5, pp. 497–507;*

[15] Zhang MJ, MJ Pomfret MJ, and Wong CM, (1996). *"Performance prediction of a backswept centrifugal impeller at off-design point conditions," International Journal for Numerical Methods in Fluids, vol. 23, no. 9, pp. 883–895.*

[16] Byskov RK, Jacobsen CB, and Pedersen N., (2003). *"Flow in a centrifugal pump impeller at design and off-design conditions—part II: large eddy simulations," ASME Journal of Fluids Engineering, vol. 125, no. 1, pp. 73–83;*

[17] Gu F., Engeda A., Cave M., and Di Liberti JL., (2001). *" A numerical investigation on the volute/diffuser interaction due to the axial distortion at the impeller exit," ASME Journal of Fluids Engineering, vol. 123, no. 3, pp. 475–483;*